HHS Public Access

Author manuscript

Mol Cell. Author manuscript; available in PMC 2016 May 31.

Published in final edited form as:

Mol Cell. 2016 May 5; 62(3): 409–421. doi:10.1016/j.molcel.2016.03.031.

The TIP60 complex regulates bivalent chromatin recognition by 53BP1 through direct H4K20me binding and H2AK15 acetylation

Karine Jacquet[1,2], **Amélie Fradet-Turcotte**[1,2,3], **Nikita Avvakumov**[1,2], **Jean-Philippe Lambert**[3], **Céline Roques**[1,2], **Raj K. Pandita**[4], **Eric Paquet**[1,2], **Pauline Herst**[1,2], **Anne-Claude Gingras**[3,5], **Tej K. Pandita**[4], **Gaëlle Legube**[6], **Yannick Doyon**[2], **Daniel Durocher**[3,5], and **Jacques Côté**[1,2,#]

[1]St-Patrick Research Group in Basic Oncology, Laval University Cancer Research Center, Oncology Axis-CHU de Québec Research Center, Hôtel-Dieu de Québec, Quebec City QC, G1R 2J6 Canada

[2]Centre Hospitalier Universitaire de Québec Research Center and School of Medicine, Laval University, Quebec City, QC, Canada.

[3]The Lunenfeld-Tanenbaum Research Institute, Mount Sinai Hospital, Toronto ON, M5G 1X5 Canada

[4]Department of Radiation Oncology, The Houston Methodist Research Institute, Houston TX, 77030 USA

[5]Department of Molecular Genetics, University of Toronto, Toronto, ON, Canada

[6]LBCMCP, Centre de Biologie Intégrative (CBI), Université de Toulouse, CNRS, UPS, France

SUMMARY

The NuA4/TIP60 acetyltransferase complex is a key regulator of genome expression and stability. Here, we identified MBTD1 as a new stable subunit of the complex and gleaned intriguing insights into TIP60's function. Harboring a histone reader domain for H4K20me1/2, MBTD1 allows TIP60 to associate with specific gene promoters and to promote the repair of DNA double strand breaks by homologous recombination. Interestingly, the non-homologous end joining factor 53BP1 engages chromatin through simultaneous binding of H4K20me2 and H2AK15ub, and it was postulated that Tip60-dependent acetylation of H4 regulates this binding. Our findings now indicate that the TIP60 complex is a potent regulator of DNA damage repair pathways in part by targeting the same histone mark as 53BP1. In addition, deposition of H2AK15ub by RNF168 inhibits chromatin acetylation by TIP60, while this residue can be acetylated by TIP60 *in vivo*, blocking its ubiquitylation. Altogether, these results uncover an intricate mechanism orchestrated by the TIP60 complex which regulates 53BP1-dependent repair pathway selection through incompatible bivalent binding and modification of chromatin.

[#]Corresponding author: (418) 525-4444 ext. 15545; ; Email: jacques.cote@crhdq.ulaval.ca

Author contributions

KJ, AFT, TKP, GL, YD, DD and JC designed the experiments. KJ, AFT, NA, JPL, CR, RKP, PH, GL and YD performed the experiments. EP analyzed the ChIP-seq/expression data. ACG supervised JPL. KJ, NA and JC wrote the manuscript.

Conflict of interest

None

Keywords

TIP60; MBTD1; NuA4; 53BP1; histone methylation; acetylation; ubiquitylation; H4K20; H2AK15; homologous recombination

INTRODUCTION

Histone post-translational modifications (PTM) act as key regulators of chromatin organization, mainly by serving as docking sites for chromatin-binding factors (Zentner and Henikoff, 2013). Acetylation of lysine residues also destabilizes the DNA-histone and histone-histone interactions, leading to a more open and dynamic chromatin organization (Steunou et al., 2014). It is catalyzed by lysine acetyltransferases such as the mammalian NuA4/TIP60 complex, a 1.5 MDa multiprotein platform of at least 16 subunits, highly conserved from yeast to human (Steunou et al., 2014). *In vivo,* TIP60's major acetylation targets are lysines (K) 5, 8 and 12 on nucleosomal H4, H2AK5, histone variants H2AZ and H2AX, as well as non-histone substrates such as p53 (Steunou et al., 2014). The TIP60 complex is a key regulator of cell homeostasis, response to stress, as well as maintenance and renewal of stem cells (Avvakumov and Cote, 2007; Voss and Thomas, 2009). It functions as an activator of transcription and is implicated in the regulation of key tumor suppressors and oncogenes such as p53, Rb and Myc (Avvakumov and Cote, 2007; Jeong et al., 2011; Kim et al., 2010; Ravens et al., 2015). Notably, Tip60/KAT5 is a haplo-insufficient tumor suppressor gene frequently mutated or deregulated in cancer (Voss and Thomas, 2009).

The NuA4/TIP60 complex also plays a key part in repair of DNA double strand breaks (DSB) (Rossetto et al., 2010). This type of DNA damage is particularly harmful as it can lead to genomic instability and loss of genetic material. Phosphorylation of Ser139 on the H2AX variant (γ-H2AX) that occurs in response to DSB initiates a cascade of signaling events and serves as a platform for recruitment of DNA repair mediators (Soria et al., 2012). Components of the NuA4/TIP60 complex are also rapidly recruited to DSB to acetylate H4, H2A and H2AX, thereby facilitating chromatin opening (Courilleau et al., 2012; Rossetto et al., 2010; Soria et al., 2012; Xu et al., 2010). Additionally, the Tip60/KAT5 acetyltransferase has been implicated in DNA damage signaling via direct acetylation and activation of ATM and inhibition of 53BP1 binding to damaged chromatin (Dantuma and van Attikum, 2016; Panier and Boulton, 2014; Tang et al., 2013). Finally, acetylation of γ-H2AX by TIP60 has been proposed to facilitate chromatin dynamics during and after DNA repair (Soria et al., 2012).

In higher eukaryotes, DSB are primarily repaired by one of two key pathways: nonhomologous end joining (NHEJ) based on the direct re-ligation of the DNA ends, and homologous recombination (HR), in which a sister chromatid is used as a template to correct damaged DNA. These two pathways are regulated by 53BP1 – a keystone of the chromatin-induced signaling pathway and a key deciding factor between HR and NHEJ (Panier and Boulton, 2014). Recruitment of 53BP1 to DNA breaks inhibits HR by blocking resection of the DNA ends and directs the repair choice to NHEJ (Panier and Boulton, 2014).

53BP1 is a bivalent chromatin reader that binds H4K20 methylation and H2AK13/15 ubiquitylation via its tandem Tudor-UDR domain. These interactions are required both for recruitment of 53BP1 to DSB and for subsequent signaling (Fradet-Turcotte et al., 2013). Since methylation of H4K20 is widely distributed in the genome, competition for H4K20me2 by JMJD2A and L3MBTL1 has been proposed to block genome-wide 53BP1 recruitment (Panier and Boulton, 2014). By contrast, ubiquitylation of H2AK13/15 is actively mediated by E3 ubiquitin-ligases RNF8/168 in response to damage (Mattiroli et al., 2012). Interestingly, recent studies directly implicate histone H4 acetylation in regulating 53BP1 during DNA damage response (DDR) and propose that TIP60-mediated H4K16ac impacts the ability of 53BP1 to bind neighboring H4K20me2 (Panier and Boulton, 2014; Tang et al., 2013).

In this study, we describe a newly identified stable subunit of the human NuA4/TIP60 acetyltransferase complex. MBTD1 contains MBT domains that recognize H4K20me and allow TIP60 to bind a number of genes, thus playing a role in regulation of transcription. Moreover, during DDR, MBTD1 regulates binding of 53BP1 at DNA lesions, likely through targeting the same H4K20me2 mark. In addition, we characterize an H2AK15 acetylation/ubiquitylation regulatory switch that further highlights the opposite functions of 53BP1 and TIP60 at DNA breaks. While RNF168-dependent H2AK15ub interferes with TIP60 binding to chromatin and blocks acetylation of H4, we demonstrate that H2AK15 can be acetylated by TIP60, inhibiting its ubiquitylation. We propose a new model in which TIP60 acts as a key regulator of DSB repair pathway choice, counterbalancing the role played by 53BP1 through incompatible bivalent interactions with chromatin near DNA lesions. Taken together, our results provide interesting insights into TIP60 function during transcription and DNA repair, and reveal a novel interplay between histone methylation, acetylation and ubiquitylation.

RESULTS

MBTD1 is a new stable subunit of the human TIP60 complex

We utilized a site-specific zinc-finger nuclease (ZFN) to effect single copy integration of a cassette containing tagged cDNA at a characterized safe harbor locus in the *PPP1R12C* gene, an integration site for the Adeno-Associated Virus (AAV)(Hockemeyer et al., 2009) (Fig. S1A). Human K562 cell line stably expressing Tip60/KAT5 was established to purify the native TIP60 complex. The integrated cassette expresses Tip60/KAT5 with a 3xFLAG tag in fusion with a 2A peptide auto-cleavage site and the puromycin resistance gene, under the control of the human *PGK1* promoter and flanked by homology sequences for the targeted integration into the AAVS1 site. The key feature of this system, other than the remarkable efficiency of integration and clonal selection, is its ability to stably express a gene at levels close to physiological, allowing large-scale purifications of different proteins under isogenic settings (Dalvai et al., 2015). Purification from nuclear extracts with stringent FLAG immunoprecipitation and peptide elution was performed and analyzed by silver staining, mass spectrometry and western blotting (Fig. 1A, Table S1). Interestingly, we detected significant amounts of the MBTD1 protein co-purifying along previously known subunits of the TIP60 complex. The same was observed when we similarly purified the

TIP60 complex via the EPC1 subunit (Fig. 1B, Table S1), and in other cell lines (HeLa and 293T, data not shown). Little is known about the function of MBTD1, other than the fact that it structurally resembles Drosophila Polycomb Group protein Sfmbt and mammalian L3MBTL1-4/SFMBT1-2, mostly due to its quadruple-repeat MBT (Malignant Brain Tumor) domain (Nady et al., 2012).

To test the specific and stable association of this protein with the TIP60 complex, we established MBTD1-3xFLAG expression in the same isogenic background, purified the MBTD1 protein and performed similar analyses (Fig. 1C-D, Table S2). These data clearly indicate that MBTD1 is exclusively associated with the same set of proteins as known TIP60 subunits. Remarkably, even histone H2AZ-H2B dimers were detected in the purified fraction, as they are involved in the histone exchange activity of the EP400/VPS72 subunits (Dalvai et al., 2015).

Thanks in part to a parallel study, we gained insights into the molecular determinants of MBTD1 association with the TIP60 complex. While studying functional domains of the EPC1 subunit based on oncogenic truncations and translocations (Avvakumov *et al.*, in preparation), we determined that MBTD1 associates with the complex through a direct interaction with EPC1. Purification of a truncated form of EPC1 (aa1-581) clearly demonstrated the normal association of all known TIP60 subunits but the specific complete loss of MBTD1 (Fig. 1E-F, Table S1). To further support these results, we performed GST pulldown assays with recombinant proteins (Fig. 1G-H, S1B). These experiments confirmed a direct interaction between the C-terminus of EPC1 and the four-MBT-domain region of MBTD1. Importantly, the presence of MBTD1 in the TIP60 complex was not found to be regulated by growth conditions or genotoxic stress, or to affect the HAT activity of the complex towards H4 and H2A on chromatin *in vitro* (Fig. S1C-D).

MBTD1 regulates binding of the TIP60 complex to specific genes *in vivo*

Previous work on MBT domains in various proteins had shown their specificity for mono- and dimethylated lysine residues, particularly H4K20 (Nady et al., 2012). Specific analysis of the MBTD1 protein revealed a preference for H4K20me1/2 (Eryilmaz et al., 2009; Nady et al., 2012), suggesting that this subunit could modulate binding of the TIP60 complex to chromatin. To address this, we first performed peptide pulldown experiments with purified GST-tagged 4MBT-repeat domain, and confirmed its robust affinity for mono- and di-methylated H4K20 (Fig. 2A). The strength of this binding is similar if not superior to that of the 53BP1 tandem Tudor domain, a well-established H4K20me-reader module, but shows a distinct preference for mono- vs. di-methylated forms (Botuyan et al., 2006; Eryilmaz et al., 2009). To test the potential impact of MBTD1 histone reader module on TIP60 HAT activity, we used recombinant nucleosome core particles carrying different levels of methylated H4K20 residue. The kinetics of *in vitro* acetylation of nucleosomes containing unmethylated H4K20 by the TIP60 complex were indistinguishable between wild type and EPC1(1-581) (i.e. lacking MBTD1) purified complexes (Fig. S2A). The same thing could be said about H4K20me1 nucleosomes, while slightly faster kinetics were detected with H4K20me2 nucleosomes in the absence of MBTD1. These results indicate that H4K20me recognition by MBTD1 has no strong effect on *in vitro* nucleosome acetylation by the TIP60 complex.

Nevertheless, contribution by MBTD1 to the function of the TIP60 complex as a tumor suppressor is supported by the strong negative effect of its overexpression on the ability of U2OS cells to form colonies (Fig. 2B, S2B), an effect slightly diminished when the predicted H4K20me-binding interface is mutated (Eryilmaz et al., 2009).

To study MBTD1 function *in vivo*, we analyzed its genome-wide location along with that of other components of the TIP60 complex. We used the different isogenic K562 cell lines to perform ChIP-seq experiments with an anti-Flag antibody, allowing standardized conditions. As implied by the complex purification data, we observed that EPC1, Tip60/KAT5 and MBTD1 significantly colocalized at the transcription start sites (TSS) of several active genes. As reported previously in yeast (Rossetto et al., 2014), the NuA4/TIP60 complex is recruited to highly transcribed genes, such as those encoding ribosomal proteins, represented here by the *RPSA* gene (Fig. 2C).

To validate our genome-wide analyses of TIP60 localization, we focused our attention on a set of 368 chromosomal regions strongly bound by at least 3 subunits unique to the complex: EPC1, Tip60/KAT5 and the newly identified MBTD1 (Fig. S2C, Table S3). Enrichment analyses on genes flanking the 368 regions indicated that the MBTD1-containing TIP60 complex is a positive regulator of transcription/protein expression, binds promoters regulated by Myc and its target genes are mostly involved in apoptosis, cell cycle regulation and hypoxia (Figure S2DE). While a link to Myc targets is expected (Kim et al., 2010), the highest correlation is detected with the BRCA1 network of transcripts. In addition, genes encoding notable regulators of cell growth, including the Rb paralog RBL1/p107 and the KMT2E/MLL5 H3K4 methyltransferase, were also found to be tightly bound by the TIP60 complex (Fig. S2F-G).

The set of 368 regions robustly bound by the TIP60 complex was then analyzed by ChIP-seq using the EPC1(1-581) mutant in order to investigate the impact of MBTD1 on TIP60's ability to target and bind chromatin *in vivo* (Fig. 2D-E, S2H, Table S3). Importantly, signals at 43% of TIP60 major targets are significantly affected in the absence of MBTD1, as exemplified by the *MAPK8IP2* promoter where we observed a complete absence of EPC1(1-581) signal compared to wild type protein. Overall, many of the genes affected by loss of MBTD1 from the complex encode proteins that function in the Aurora B kinase pathway (data not shown). In addition, we used CRISPR/Cas9 technology to produce MBTD1 knockout cells (U2OS, see below) and performed genome-wide expression analysis on three different clones compared to wild type cells (Tables S4-S7). Importantly, downregulated genes in the absence of MBTD1 tend to carry the H4K20me1 histone mark, to be bound by Myc and are similar to the ones affected by the loss of BRCA1. Collectively, our results demonstrate that MBTD1 is a stable near stoichiometric subunit of the TIP60 complex, with important contribution to its function in transcription and to proper association of the complex with a subset of genomic loci.

MBTD1 is a regulator of DNA damage response within the TIP60 complex

The NuA4/TIP60 complex is a well-established regulator of DNA damage response in organisms ranging from yeast to human (Dantuma and van Attikum, 2016; Rossetto et al., 2010). Since Tip60/KAT5 is directly recruited at DSB in human cells (Murr et al., 2006), we

tested by ChIP if we could also detect MBTD1 recruitment at inducible breaks using ZFN targeting the *AAVS1* locus (Xu et al., 2010). As shown in figure 3A, we could detect appearance of TIP60 subunits MBTD1 and EPC1 close to the DNA break induced *in vivo* by the nuclease. This result was also reproduced using the AsiS1-DIvA inducible system (Fig. S3B)(Aymard et al., 2014). Tip60/KAT5 had been previously reported to affect removal of γ-H2AX foci after DNA damage (Sharma et al., 2010; Soria et al., 2012), we performed comparable experiments to determine whether depletion of MBTD1 could influence the kinetics of γ-H2AX foci formation and disappearance after cell irradiation. First, we analyzed knockdowns of two other important subunits of TIP60, EP400 and ING3, and saw a similar effect to what we had previously observed with Tip60 depletion (Sharma et al., 2010). In all three cases, loss of TIP60 subunits led to normal rapid appearance of γ-H2AX foci after irradiation, but a robust persistence of these foci for several hours after DNA damage compared to wild type cells (Fig. S3C). This is in clear contrast to knockdown of MOF/KAT8, which is responsible for the bulk of H4K16 acetylation and delays formation of γ-H2AX foci but not their removal (Sharma et al., 2010). In similar experiments, MBTD1 knockdown completely phenocopies depletion of Tip60, ING3 and EP400 in U2OS and 293 cells (Fig. 3B and S3D). This persistence of γ-H2AX foci reflects an inability to destabilize them in the absence of TIP60 activity (Soria et al., 2012) but also an actual defect in DNA repair (Murr et al., 2006; Rossetto et al., 2010). Thus, we used two *in vivo* reporter systems for either HR or NHEJ in order to study the impact of Tip60/KAT5 and MBTD1 knockdowns on DSB repair (Sharma et al., 2010). MBTD1 knockdown, like previously reported for Tip60/KAT5 and PALB2, significantly decreased repair by HR (Fig. 3C). In stark contrast, the complementary reporter system showed better repair by NHEJ in the absence of Tip60 or MBTD1 (Fig. 3D). These effects are not a simple consequence of changes in cell cycle distribution during depletion (Fig. S3F). Furthermore, we performed a rescue experiment in the HR reporter system with siRNA-resistant expression of WT MBTD1 and the MBT4 triple mutant (Fig. 3E). WT MBTD1 can fully rescue the loss of repair by HR with siMBTD1 while the mutant also rescued but not as efficiently. Interestingly, overexpression of WT and mutant MBTD1 seemed to have dominant opposing effect on HR in the absence of knockdown. Altogether, these results indicate that MBTD1, like Tip60, is critical for the function of the TIP60 complex in facilitating repair of DSBs, specifically through HR (Courilleau et al., 2012; Murr et al., 2006; Tang et al., 2013).

Tip60 and MBTD1 regulate the dynamics of 53BP1 binding near DNA damage

H4 acetylation and the TIP60 complex have been implicated in inhibition of 53BP1 binding to damaged chromatin (Tang et al., 2013). Additionally, both MBTD1 and 53BP1 have chromatin reader modules specific for H4K20me2. Given these facts, we logically speculated that MBTD1 could affect the dynamics of 53BP1 localization at DSBs and thus regulate DNA damage response. We first asked whether MBTD1 could efficiently compete with 53BP1 for binding to H4K20me2 *in vitro* (Fig. 4A). To test this, we saturated biotinylated H4K20me2 peptides with purified Tudor domain of 53BP1, bound these complexes to streptavidin resin, and then added increasing amounts of the purified MBT repeat domain of MBTD1. The MBTD1 reader module was able to partly displace 53BP1 Tudor domain from H4K20me2 peptides starting at a ratio of 1:1 between the two domains. This supports the hypothesis that MBTD1 within the TIP60 complex competes with 53BP1

for binding to H4K20me2-bearing chromatin near DNA breaks and helps repair pathway choice.

We then assessed the dynamics of 53BP1 foci formation and disappearance by performing immunofluorescence analyses after cell irradiation (Fig. 4B-E and S4). We observed that knockdowns of Tip60/KAT5 or MBTD1 did not affect formation of 53BP1 foci after DNA damage, just as they had not affected appearance of γ-H2AX foci. However, depletion of Tip60/KAT5 and MBTD1 clearly delayed removal of 53BP1 foci, as evidenced by their persistence 5 hours after irradiation. These results suggest that binding of MBTD1 to the H4K20me histone mark does not appear to compete with 53BP1 during the latter's initial recruitment to DNA breaks. The same can be said about the TIP60 complex and its acetyltransferase activity toward the H4 tail. However, MBTD1/TIP60 do regulate persistence of 53BP1 after its initial recruitment, most likely during the critical stage when 53BP1 needs to be displaced to allow DNA end resection and HR. This is also probably linked to TIP60-dependent acetylation and removal of γ-H2AX to increase chromatin dynamics, allowing resection and loading of Rad51 (Courilleau et al., 2012; Murr et al., 2006; Soria et al., 2012).

To get a more definite answer on the interplay between MBTD1 and 53BP1 at DSB, we used CRISPR/Cas9 to produce MBTD1 KO cell lines (U2OS). We integrated by DSB-mediated HR stop codons/frameshift a few codons downstream of the ATG and isolated multiple homozygote KO clones confirmed by PCR-digestion and sequencing (Fig. S5A-B). These clones were used in microarray expression experiments described above and the transcription profiles cluster together. Asynchronous cell populations show cell cycle profiles similar to wild type cells but release after thymidine block presents a slower progression through S/G2 (Fig. S5C). Using these KO cells we then measured DNA repair efficiency after etoposide treatment by Comet assay (Fig. 5A). Results indicate that MBTD1 KO cells are significantly less efficient at repairing DNA breaks. Western blot analysis 0, 1 and 6h after etoposide treatment also shows significantly increased phosphorylation of RPA, and altered 53BP1 phosphorylation kinetics in MBTD1 KO cells (Fig. S5D).

We then used these KO cell lines to assess the dynamics of 53BP1 foci formation and disappearance by immunofluorescence after cell irradiation (Fig. 5B-F). Cells lacking MBTD1 confirm the persistence of 53BP1 foci 5h after damage. Strikingly, they also clearly show more 53BP1 foci formed 1h post irradiation. These data argue that MBTD1 can block binding of 53BP1 to DNA damage sites. This concept was supported by rescue experiments performed in the MBTD1 KO cells (Fig. 5E-F). Expression of MBTD1 by transient transfection in the KO cell lines drastically brought down the number of 53BP1 foci detected both 1 and 5h after irradiation. Interestingly, it even lowered the numbers of foci in wild type cells, suggesting that MBTD1 over-expression can partly block binding of 53BP1 to DNA damage sites.

A switch between ubiquitylation and acetylation of H2AK15 can regulate the opposing functions of 53BP1 and TIP60

Since binding to H4K20me and acetylation of the H4 tail by the TIP60 complex can modulate 53BP1 binding to sites of DNA damage, we next turned our attention to the N-

terminus of H2A as it is critical for 53BP1 association with chromatin. DNA damage-induced RNF168-dependent ubiquitylation of H2AK15 even supersedes H4K20me in *in vitro* chromatin binding assays with 53BP1's UDR domain (Fradet-Turcotte et al., 2013). Interestingly, the NuA4/TIP60 subunit EPC1 is required for nucleosome binding and H4 tail acetylation by the complex, through a direct interaction between the first 12 amino acids of EPC1 and the N-terminal tail of histone H2A (Chittuluru et al., 2011; Huang and Tan, 2013; Lalonde et al., 2013). Therefore, we speculated that RNF168-dependent ubiquitylation of H2AK15 has a direct impact on TIP60's ability to acetylate the H4 tail and modulate 53BP1 binding. To test this hypothesis, we used recombinant RNF168 to ubiquitylate purified native nucleosomes *in vitro* (Fig. S6A). We then used these nucleosomes as a substrate for *in vitro* acetylation assays with purified TIP60 complex and observed that H2AK15 ubiquitylation selectively blocked acetylation (Fig. 6A). This inhibition is specific as it did not occur with another histone H4-specific HAT complex, HBO1-JADE1-ING4 (Lalonde et al., 2013), that targets the same residues but needs to bind the H3 tail instead of H2A in order to acetylate nucleosomes (Saksouk et al., 2009).

In parallel, since NuA4/TIP60 is known to acetylate the N-terminal tail of H2A on lysines 5 and 9 *in vitro* and *in vivo* (Steunou et al., 2014), it was interesting to verify whether H2AK15 itself could also be acetylated *in vivo* and whether TIP60 was involved. In addition, H2A residues targeted by RNF168 for ubiquitylation, K13 and K15, have also been found acetylated *in vivo* (Zheng et al., 2013). Since lysine acetylation and ubiquitylation are mutually exclusive, we speculated that acetylation of H2AK15, potentially by the TIP60 complex, could be an additional mechanism of regulating 53BP1 binding to chromatin. To address this question, we first demonstrated that we could detect the acetylation of H2AK15 on native chromatin by western blotting with a specific antibody, and that incubation with the TIP60 complex and acetyl-CoA increases this signal, similar to what is seen with H4 acetylation (Fig. S6B). To validate the H2AK15ac antibody, we then incubated wild type and mutant recombinant nucleosomes with purified TIP60 complex and detected a specific H2AK15ac signal, which is completely lost when K15 is mutated (Fig. 6B). Importantly, a K13 mutant does not affect the TIP60-dependent signal detected by the antibody, while a H4Kc20me2 analog-bearing nucleosome does not stimulate it.

In addition, overexpression *in vivo* (293T cells) of the nucleosomal HAT core of the TIP60 complex, termed piccolo-TIP60 (Tip60+EPC1+ING3), led to a dramatic increase in acetylation of H2AK15 as well as of other histone substrates (Fig. 6C and S6C). More importantly, knockdown experiments using siRNAs show a clear decrease of H2AK15ac signal in vivo in the absence of Tip60, demonstrating that this is a new *bone fide* acetylation target of the complex (Fig. 6D). It was also interesting to test whether the presence of the MBTD1 subunit could contribute to acetylation of H2AK15 by TIP60. However, experiments using native purified complexes or analysis of MBTD1 KO cell lines did not show any variation in H2AK15 acetylation levels *in vitro* or *in vivo* (Fig. S6D-E).

Interestingly, we analyzed H2AK15ac signals throughout the cell cycle and observed an enrichment of this mark in G2/M (Fig. 6E and S6F). This potentially correlates with HR in early G2, as well as with the necessary release of 53BP1 from chromatin during mitosis (Orthwein et al., 2014). To test whether acetylation of H2AK15 could be linked to DNA

damage response, we analyzed by western blotting bulk histones extracted 1hr after treatment with the DNA damaging agent etoposide. We observed a global deacetylation of histones H3 and H4, as well as of H2AK5 (Fig. 6F). In sharp contrast, H2AK15ac did not show such a decrease and instead appeared to increase slightly. In parallel, we performed immunofluorescence with the anti-H2AK15ac antibody on irradiated cells (Fig. 6G). The images revealed a global increase of the H2AK15ac signal on chromatin after irradiation, but not particularly enriched near γ-H2AX foci. After normalizing the signals in each cell with the DAPI signal, it became apparent that H2AK15ac increase significantly through the nuclei 1h after irradiation and goes back to normal after 5h (Fig. 6H). These results indicate that acetylation of H2AK15 is specifically regulated in response to DNA damage, in a very distinct manner compared to other modifications. They also suggest that H2AK15ac could play a role in restricting H2AK15 ubiquitylation by RNF168 to the vicinity of the DNA breaks (Gudjonsson et al., 2012). siRNA experiments indicate that the DNA damage-induced H2AK15ac signal is also dependent on Tip60, but results after depletion of RNF168 are difficult to interpret (Fig. 6H). Altogether, these data implicate the TIP60 complex in an ubiquitylation/acetylation switch at H2AK15 that regulates the function of 53BP1 during DNA damage repair.

Since immunofluorescence showed a more general increase of nuclear H2AK15ac in response to DNA damage, we turned to ChIP analysis at inducible DNA breaks to question its dynamics near DSB. Using the ER-AsiS1 DIvA system, we could investigate different DSB that were previously characterized to be preferentially repaired by HR or NHEJ (Aymard et al., 2014). Our first attempts on asynchronous cells did not show an increase of H2AK15ac at any DSB, but rather a slight decrease (Fig. S7A). On the other hand, it was obvious that location prone to be repaired by HR were drastically more enriched in H2AK15ac even before DSB formation, suggesting a link with transcriptionally active chromatin. We then synchronized the cells in G1 or S/G2 before ChIPs to verify if phases of the cell cycle could differentially implicate H2AK15ac at DSB (Fig. 7A-B and S7B-C). Interestingly, an increase of H2AK15ac is detected at DNA breaks specifically in S/G2 and only at sites preferentially repaired by HR. However, in G1 cells, these same DSB sites showed a decrease of H2AK15ac, arguing that TIP60 function at DSB is predominant in S/G2. In parallel, DSB sites that are preferentially repaired by NHEJ (and preferentially located in non-transcriptionally active regions) showed stable very low levels of H2AK15ac in both G1 and S/G2.

DISCUSSION

Activities of the multifunctional TIP60/NuA4 complex are modulated by a number of internal motifs capable of reading histone marks. Subunits of the complex contain domains that individually are capable of binding histone PTM in distinct genomic contexts (Fig. 7C). Thus, it is crucial to consider the TIP60 complex as a whole in order to fully understand any of its functions. Furthermore, conducting experiments in conditions close to physiological is essential as true histone target specificity is often only achieved with native modifying or remodeling complexes and their *bona fide* chromatin substrates (Lalonde et al., 2014).

In this study, we identified MBTD1 as a new stable stoichiometric subunit of the TIP60 complex, with which it appears to be exclusively associated. This protein can read histone PTM through its quadruple MBT repeat and displays a strong affinity for H4K20me1/2 (K_D 7-13 μM) (Eryilmaz et al., 2009). Our discovery of the physical association between MBTD1 and TIP60 can reconcile contradictory observations about the role of H4K20me1 and the enzyme responsible for its deposition, SETD8. Prior studies had predominantly linked them to gene repression. This conclusion had been reached mainly through work on the L3MBTL1/2 transcription repressors that also contain H4K20me1/2-specific MBT repeats (van Nuland and Gozani, 2015). Inexplicably, ChIP-seq analysis of H4K20me1 had demonstrated a relatively high occupancy of this histone mark within bodies of actively transcribed genes (Ernst et al., 2011). Furthermore, mass spectrometry analysis had uncovered a frequent co-occurrence of transcriptionally permissive acetylated lysines and K20me1/2 within the tails of the same histone molecules (Pesavento et al., 2008). Our present discovery of the MBTD1-TIP60 association finally establishes a clear link between H4K20me1/2 and transcription activation. It will be interesting to investigate whether this connection is responsible for the role of H4K20me1 in local regulation of RNA polymerase II pausing through targeted H4 acetylation (Kapoor-Vazirani and Vertino, 2014).

Both the TIP60 complex and H4K20me are important players in the cellular response to DNA double strand breaks. H4K20 methylation at DSB is rapidly recognized by the double Tudor domain of 53BP1 (Botuyan et al., 2006). Other H4K20me readers, L3MBTL1 and JMJD2A/KDM4A, are actively displaced to allow 53BP1 to bind damaged chromatin (Panier and Boulton, 2014). Acetylation of the H4 tail by Tip60/KAT5 has been hypothesized to disrupt the interaction of 53BP1's tandem Tudor domain with the neighboring H4K20me2 (Panier and Boulton, 2014; Tang et al., 2013). Interestingly, budding yeast KAT5/Esa1 performs an opposite function to that of the 53BP1 homolog Rad9 in controlling the cell cycle upon DNA damage (Javaheri et al., 2006). However, budding yeast lacks H4K20 methylation, which may explain the absence of an MBTD1 homolog in the yeast NuA4 complex.

Given the above, it was intriguing to investigate a possible role of MBTD1 in the cellular response to DNA damage. Our results presented demonstrate that MBTD1 can displace 53BP1 for the H4K20me2 mark *in vitro* and affect the formation and stability of 53BP1 foci after DNA damage *in vivo*. MBTD1 and TIP60 regulate the disappearance of these foci at a later time-point after damage – a process that mirrors TIP60's role in removing γ-H2AX foci within a similar time frame. These activities are clearly important for repair of DSB by homologous recombination, as TIP60 is required for efficient loading of Rad51 (Courilleau et al., 2012; Murr et al., 2006). Thus, our observations favor the model in which the TIP60 complex promotes HR repair over NHEJ by decreasing 53BP1 occupancy on damaged chromatin, thereby relieving inhibition of DNA end resection and homology search (Panier and Boulton, 2014; Tang et al., 2013).

We show that the EPC1 subunit of TIP60 is responsible for the direct association of MBTD1 with the complex. In addition, EPC1 interacts with the N-terminal tail of histone H2A in the nucleosome, which is critical for H4 acetylation by TIP60 (Huang and Tan, 2013; Lalonde et al., 2013). This led us to investigate whether TIP60 and 53BP1 also vie for chromatin

interaction via the H2A tail. DNA damage-induced ubiquitylation of H2A on K13 and K15 by RNF168 is critical for 53BP1 binding through its UDR domain, as well as for signaling (Fradet-Turcotte et al., 2013). In this study, we show that while H2AK15ub nucleosomes are refractory to modification by TIP60, acetylation of H2AK15 is induced *in vivo* in response to DNA damage. This ubiquitylation/acetylation switch is clearly a powerful mechanism of regulating 53BP1 binding and TIP60-dependent histone H4 acetylation. Taken together, our observations of the events surrounding H4K20me demonstrate distinctly incompatible binding and opposing functions of 53BP1 and TIP60/NuA4 on nucleosomes near DNA lesions (Fig. 7D).

53BP1 is a bivalent chromatin reader, binding both H2AK15ub and H4K20me2 via its Tudor and UDR regions. Strikingly, TIP60 targets the same two nucleosome surfaces through MBTD1 and EPC1. If TIP60 gains the upper hand in binding nucleosomes near DNA breaks, local acetylation of the H4 tail further blocks 53BP1 binding, as proposed previously (Tang et al., 2013). Naturally, activities of deacetylases and de-ubiquitinases of H2AK15 are critical in shifing the balance between 53BP1 and TIP60. This is consistent with the established model in which HDAC1/2 promote end joining of DSB, likely by negating the activity of TIP60 (Miller et al., 2010). Importantly, acetylation of H2AK15 after DNA damage is induced throughout the nucleus and not only in the vicinity of DSBs. We hypothesize that this may serve to block promiscuous ubiquitylation of H2A by RNF168, which is induced as part of the repair process, restricting it to the vicinity of DNA lesions (Gudjonsson et al., 2012). Likewise, increased levels of H2AK15ac in the G2/M phase of the cell cycle may be linked to homologous recombination, but may also block unwanted DSB repair during mitosis (Orthwein et al., 2014).

Overall, the identification of MBTD1 as a stable subunit of the TIP60 complex raises several interesting questions. The putative oncogenicity of several translocations or truncations of EPC1, found in uterine sarcoma and leukemia, could be partly explained by the loss of MBTD1 from the complex (Avvakumov and Cote, 2007). It will also be very interesting to investigate the function of MBTD1 in gene regulation and chromatin dynamics *vis-a-vis* other H4K20me readers like the L3MBTL1/2 repressors. Furthermore, both 53BP1 and L3MBTL1 can bind specific mono- and di-methylated lysines on tumor suppressors p53, thereby regulating its function (Kachirskaia et al., 2008; West et al., 2010). Thus, it will be important to examine whether MBTD1 can also target such non-histone proteins and counteract their inhibition. Finally, 53BP1 itself is acetylated *in vivo* on multiple lysine residues, including those near the UDR domain and within the dimerization domain (phosphosite.org). Therefore, it will be intriguing to determine whether these modifications are carried out by TIP60 to further regulate 53BP1 function in the cellular response to DNA damage.

In conclusion, our findings reveal new insights about TIP60 composition, architecture and function during transcription and DNA repair. Notably, our data further uncover the role in repair pathway choice played by TIP60 through multivalent interactions and chromatin modifications at DNA breaks. This study highlights the intricate crosstalk between acetylation, methylation and ubiquitylation of chromatin in proper coordination of DSB repair. Retention of 53BP1 on damaged chromatin appears to be the key element in the

decision between HR and NHEJ. Therefore, the incompatibility between TIP60 and 53BP1 is instrumental in the temporal and spatial orchestration of DSB repair, which relies on complex and finely modulated interactions between a variety of chromatin post-translational modifications.

EXPERIMENTAL PROCEDURES

Establishment of isogenic cell lines expressing TIP60 components from the *AAVS1* safe harbor and MBTD1 KO cell lines using CRISPR/Cas9

K562 cells were used to express components of the TIP60 complex from the AAVS1 safe harbor using ZFN-mediated insertion/recombination as described (Dalvai et al., 2015). MBTD1 KO was produced in U2OS cells using CRISPR/Cas9 also similar to what we previously described (Dalvai et al., 2015). Technical details and information about genome-wide expression analysis of MBTD1 KO cells are provided in supplemental experimental procedures.

Purification of native HAT complexes

Native TIP60 complexes were purified essentially as described before (Dalvai et al., 2015) with some modifications detailed in supplemental experimental procedures. Information about mass spectrometry analysis, antibodies and RNAi reagents is also provided in supplemental experimental procedures.

ChIP and ChIP-seq libraries

ChIP-seq experiments and analysis with K562 cells were performed as previously described (Lalonde et al., 2013) with minor modifications detailed in supplemental experimental procedures. For ChIP at a DSB induced in the *AAVS1* locus using ZFN, previously described 3xFLAG-tagged EPC1 and MBTD1 K562 cell lines produced by CRISPR-mediated tagging of endogenous genes were used (Dalvai et al., 2015). Briefly, cells were transfected by Amaxa 4DNucleofector (Lonza) with ZFN for 18h followed by FLAG ChIP as described above. For H2AK15ac and γ-H2AX ChIP at AsiSI-dependent DSB, the AID-DIvA Flag empty cell line was synchronized by double thymidine block and processed as described in (Aymard et al., 2014). ChIP conditions and primers are provided in supplemental experimental procedures.

In vitro and *in vivo* functional assays

Information about the purification of chromatin, histones, recombinant proteins, pull-downs, histone acetylation and ubiquitylation assays is provided in supplemental experimental procedures. Detailed information about the conditions used for immunofluorescence of γ-H2AX/53BP1 foci after cell irradiation, H2AK15ac/DAPI intensity analysis, reporter cell lines for HR/NHEJ measurements, COMET assay and cell cycle analysis is also provided in supplemental experimental procedures.

Supplementary Material

Refer to Web version on PubMed Central for supplementary material.

Acknowledgments

We are grateful to members of the Côté and Durocher labs as well as Roger Greenberg for helpful discussions. We are also in debt to Yvan Canitrot and Didier Trouche for advice, discussion and sharing preliminary data. We thank Matthew Porteus for NHEJ/HR reporter plasmids, Valerie Côté for FACS analysis, Lianne Dale (Leica Microsystems) for technical support and Laval University/Compute Canada for the use of supercomputers. This work was supported by grants from: the Canadian Institutes of Health Research (CIHR) to A.-C.G. (MOP-123322), D.D. (FDN-143343) and J.C. (MOP-64289, FDN-334002); the Natural Sciences and Engineering Research Council of Canada (NSERC) to Y.D. (RGPIN-2014-059680); the European Research Council (ERC-2014-CoG 647344), Agence Nationale pour la Recherche (ANR-14-CE10-0002-01 and ANR-13-BSV8-0013), and the Ligue Nationale contre le Cancer (LNCC) to G.L.; and the National Institutes of Health (NIH) to T.K.P. (CA129537, CA154320, and GM109768).

K.J was supported by PhD studentships from Laval University Faculty of Medicine and Fonds Québécois de la Recherche sur la Nature et les Technologies. A.F.-T. and J.-P.L were supported by post-doctoral fellowships from the CIHR and J.-P.L. also by a TD Bank Health Research Fellowship at the Lunenfeld-Tanenbaum Research Institute. A.-C.G. holds the Canada Research Chair in Functional Proteomics and the Lea Reichmann Chair in Cancer Proteomics. Y.D. is junior 1 scholar from the Fonds de la Recherche du Québec-Santé (FRQS). D.D. holds the Canada Research Chair in the Molecular Mechanisms of Genome Integrity and J.C. the Canada Research Chair in Chromatin Biology and Molecular Epigenetics.

REFERENCES

Avvakumov N, Cote J. The MYST family of histone acetyltransferases and their intimate links to cancer. Oncogene. 2007; 26:5395–5407. [PubMed: 17694081]

Aymard F, Bugler B, Schmidt CK, Guillou E, Caron P, Briois S, Iacovoni JS, Daburon V, Miller KM, Jackson SP, et al. Transcriptionally active chromatin recruits homologous recombination at DNA double-strand breaks. Nat Struct Mol Biol. 2014; 21:366–374. [PubMed: 24658350]

Botuyan MV, Lee J, Ward IM, Kim JE, Thompson JR, Chen J, Mer G. Structural basis for the methylation state-specific recognition of histone H4-K20 by 53BP1 and Crb2 in DNA repair. Cell. 2006; 127:1361–1373. [PubMed: 17190600]

Chittuluru JR, Chaban Y, Monnet-Saksouk J, Carrozza MJ, Sapountzi V, Selleck W, Huang J, Utley RT, Cramet M, Allard S, et al. Structure and nucleosome interaction of the yeast NuA4 and Piccolo-NuA4 histone acetyltransferase complexes. Nat Struct Mol Biol. 2011; 18:1196–1203. [PubMed: 21984211]

Courilleau C, Chailleux C, Jauneau A, Grimal F, Briois S, Boutet-Robinet E, Boudsocq F, Trouche D, Canitrot Y. The chromatin remodeler p400 ATPase facilitates Rad51-mediated repair of DNA double-strand breaks. J Cell Biol. 2012; 199:1067–1081. [PubMed: 23266955]

Dalvai M, Loehr J, Jacquet K, Huard CC, Roques C, Herst P, Cote J, Doyon Y. A Scalable Genome-Editing-Based Approach for Mapping Multiprotein Complexes in Human Cells. Cell reports. 2015; 13:621–633. [PubMed: 26456817]

Dantuma NP, van Attikum H. Spatiotemporal regulation of posttranslational modifications in the DNA damage response. EMBO J. 2016; 35:6–23. [PubMed: 26628622]

Ernst J, Kheradpour P, Mikkelsen TS, Shoresh N, Ward LD, Epstein CB, Zhang X, Wang L, Issner R, Coyne M, et al. Mapping and analysis of chromatin state dynamics in nine human cell types. Nature. 2011; 473:43–49. [PubMed: 21441907]

Eryilmaz J, Pan P, Amaya MF, Allali-Hassani A, Dong A, Adams-Cioaba MA, Mackenzie F, Vedadi M, Min J. Structural studies of a four-MBT repeat protein MBTD1. PLoS One. 2009; 4:e7274. [PubMed: 19841675]

Fradet-Turcotte A, Canny MD, Escribano-Diaz C, Orthwein A, Leung CC, Huang H, Landry MC, Kitevski-LeBlanc J, Noordermeer SM, Sicheri F, et al. 53BP1 is a reader of the DNA-damage-induced H2A Lys 15 ubiquitin mark. Nature. 2013; 499:50–54. [PubMed: 23760478]

Gudjonsson T, Altmeyer M, Savic V, Toledo L, Dinant C, Grofte M, Bartkova J, Poulsen M, Oka Y, Bekker-Jensen S, et al. TRIP12 and UBR5 suppress spreading of chromatin ubiquitylation at damaged chromosomes. Cell. 2012; 150:697–709. [PubMed: 22884692]

Hockemeyer D, Soldner F, Beard C, Gao Q, Mitalipova M, DeKelver RC, Katibah GE, Amora R, Boydston EA, Zeitler B, et al. Efficient targeting of expressed and silent genes in human ESCs and iPSCs using zinc-finger nucleases. Nat Biotechnol. 2009; 27:851–857. [PubMed: 19680244]

Huang J, Tan S. Piccolo NuA4-catalyzed acetylation of nucleosomal histones: critical roles of an Esa1 Tudor/chromo barrel loop and an Epl1 enhancer of polycomb A (EPcA) basic region. Mol Cell Biol. 2013; 33:159–169. [PubMed: 23109429]

Javaheri A, Wysocki R, Jobin-Robitaille O, Altaf M, Cote J, Kron SJ. Yeast G1 DNA damage checkpoint regulation by H2A phosphorylation is independent of chromatin remodeling. Proc Natl Acad Sci U S A. 2006; 103:13771–13776. [PubMed: 16940359]

Jeong KW, Kim K, Situ AJ, Ulmer TS, An W, Stallcup MR. Recognition of enhancer element-specific histone methylation by TIP60 in transcriptional activation. Nat Struct Mol Biol. 2011; 18:1358–1365. [PubMed: 22081016]

Kachirskaia I, Shi X, Yamaguchi H, Tanoue K, Wen H, Wang EW, Appella E, Gozani O. Role for 53BP1 Tudor domain recognition of p53 dimethylated at lysine 382 in DNA damage signaling. J Biol Chem. 2008; 283:34660–34666. [PubMed: 18840612]

Kapoor-Vazirani P, Vertino PM. A dual role for the histone methyltransferase PR-SET7/SETD8 and histone H4 lysine 20 monomethylation in the local regulation of RNA polymerase II pausing. J Biol Chem. 2014; 289:7425–7437. [PubMed: 24459145]

Kim J, Woo AJ, Chu J, Snow JW, Fujiwara Y, Kim CG, Cantor AB, Orkin SH. A Myc network accounts for similarities between embryonic stem and cancer cell transcription programs. Cell. 2010; 143:313–324. [PubMed: 20946988]

Lalonde ME, Avvakumov N, Glass KC, Joncas FH, Saksouk N, Holliday M, Paquet E, Yan K, Tong Q, Klein BJ, et al. Exchange of associated factors directs a switch in HBO1 acetyltransferase histone tail specificity. Genes Dev. 2013; 27:2009–2024. [PubMed: 24065767]

Lalonde ME, Cheng X, Cote J. Histone target selection within chromatin: an exemplary case of teamwork. Genes Dev. 2014; 28:1029–1041. [PubMed: 24831698]

Mattiroli F, Vissers JH, van Dijk WJ, Ikpa P, Citterio E, Vermeulen W, Marteijn JA, Sixma TK. RNF168 ubiquitinates K13-15 on H2A/H2AX to drive DNA damage signaling. Cell. 2012; 150:1182–1195. [PubMed: 22980979]

Miller KM, Tjeertes JV, Coates J, Legube G, Polo SE, Britton S, Jackson SP. Human HDAC1 and HDAC2 function in the DNA-damage response to promote DNA nonhomologous end-joining. Nat Struct Mol Biol. 2010; 17:1144–1151. [PubMed: 20802485]

Murr R, Loizou JI, Yang YG, Cuenin C, Li H, Wang ZQ, Herceg Z. Histone acetylation by Trrap-Tip60 modulates loading of repair proteins and repair of DNA double-strand breaks. Nat Cell Biol. 2006; 8:91–99. [PubMed: 16341205]

Nady N, Krichevsky L, Zhong N, Duan S, Tempel W, Amaya MF, Ravichandran M, Arrowsmith CH. Histone recognition by human malignant brain tumor domains. J Mol Biol. 2012; 423:702–718. [PubMed: 22954662]

Orthwein A, Fradet-Turcotte A, Noordermeer SM, Canny MD, Brun CM, Strecker J, Escribano-Diaz C, Durocher D. Mitosis inhibits DNA double-strand break repair to guard against telomere fusions. Science. 2014; 344:189–193. [PubMed: 24652939]

Panier S, Boulton SJ. Double-strand break repair: 53BP1 comes into focus. Nat Rev Mol Cell Biol. 2014; 15:7–18. [PubMed: 24326623]

Pesavento JJ, Yang H, Kelleher NL, Mizzen CA. Certain and progressive methylation of histone H4 at lysine 20 during the cell cycle. Mol Cell Biol. 2008; 28:468–486. [PubMed: 17967882]

Ravens S, Yu C, Ye T, Stierle M, Tora L. Tip60 complex binds to active Pol II promoters and a subset of enhancers and co-regulates the c-Myc network in mouse embryonic stem cells. Epigenetics & chromatin. 2015; 8:45. [PubMed: 26550034]

Rossetto D, Cramet M, Wang AY, Steunou AL, Lacoste N, Schulze JM, Cote V, Monnet-Saksouk J, Piquet S, Nourani A, et al. Eaf5/7/3 form a functionally independent NuA4 submodule linked to RNA polymerase II-coupled nucleosome recycling. EMBO J. 2014; 33:1397–1415. [PubMed: 24843044]

Rossetto D, Truman AW, Kron SJ, Cote J. Epigenetic modifications in double-strand break DNA damage signaling and repair. Clinical cancer research : an official journal of the American Association for Cancer Research. 2010; 16:4543–4552. [PubMed: 20823147]

Saksouk N, Avvakumov N, Champagne KS, Hung T, Doyon Y, Cayrou C, Paquet E, Ullah M, Landry AJ, Cote V, et al. HBO1 HAT complexes target chromatin throughout gene coding regions via multiple PHD finger interactions with histone H3 tail. Mol Cell. 2009; 33:257–265. [PubMed: 19187766]

Sharma GG, So S, Gupta A, Kumar R, Cayrou C, Avvakumov N, Bhadra U, Pandita RK, Porteus MH, Chen DJ, et al. MOF and histone H4 acetylation at lysine 16 are critical for DNA damage response and double-strand break repair. Mol Cell Biol. 2010; 30:3582–3595. [PubMed: 20479123]

Soria G, Polo SE, Almouzni G. Prime, repair, restore: the active role of chromatin in the DNA damage response. Mol Cell. 2012; 46:722–734. [PubMed: 22749398]

Steunou, A-L.; Rossetto, D.; Cote, J. Regulating Chromatin by Histone Acetylation. In: Workman, JL.; Abmayr, SM., editors. Fundamentals of Chromatin. Springer; New York: 2014. p. 147-212.

Tang J, Cho NW, Cui G, Manion EM, Shanbhag NM, Botuyan MV, Mer G, Greenberg RA. Acetylation limits 53BP1 association with damaged chromatin to promote homologous recombination. Nat Struct Mol Biol. 2013; 20:317–325. [PubMed: 23377543]

van Nuland R, Gozani O. H4K20 methylation: expanding the signaling potential of the proteome one methyl moiety at a time. Molecular & cellular proteomics : MCP. 2015

Voss AK, Thomas T. MYST family histone acetyltransferases take center stage in stem cells and development. BioEssays : news and reviews in molecular, cellular and developmental biology. 2009; 31:1050–1061.

West LE, Roy S, Lachmi-Weiner K, Hayashi R, Shi X, Appella E, Kutateladze TG, Gozani O. The MBT repeats of L3MBTL1 link SET8-mediated p53 methylation at lysine 382 to target gene repression. J Biol Chem. 2010; 285:37725–37732. [PubMed: 20870725]

Xu Y, Sun Y, Jiang X, Ayrapetov MK, Moskwa P, Yang S, Weinstock DM, Price BD. The p400 ATPase regulates nucleosome stability and chromatin ubiquitination during DNA repair. J Cell Biol. 2010; 191:31–43. [PubMed: 20876283]

Zentner GE, Henikoff S. Regulation of nucleosome dynamics by histone modifications. Nat Struct Mol Biol. 2013; 20:259–266. [PubMed: 23463310]

Zheng Y, Thomas PM, Kelleher NL. Measurement of acetylation turnover at distinct lysines in human histones identifies long-lived acetylation sites. Nat Commun. 2013; 4:2203. [PubMed: 23892279]

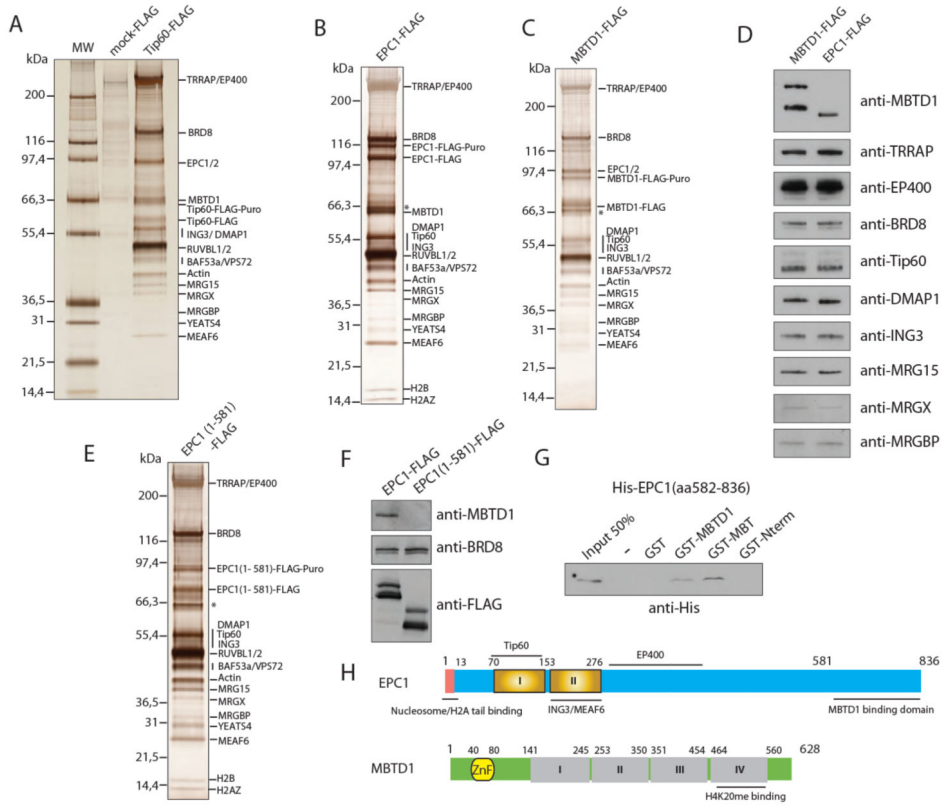

Figure 1. MBTD1 is a stable subunit of the human TIP60/NuA4 acetyltransferase complex

(A) Purification of native TIP60/NuA4 complex from K562 cells. The TIP60 complex was purified using a K562 cell line modified to stably express Tip60-3xFLAG (Fig. S1A). Anti-FLAG immunoprecipitation was performed on nuclear extract, bound material was then eluted with 3xFLAG peptide and analyzed on 4-12% SDS-PAGE followed by silver staining. A mock purification was performed on a control cell line expressing an empty 3xFLAG tag. Subunits were identified by western blotting and mass spectrometry (Tables S1-S2). **(B-C)** Purification of native TIP60 complexes from K562 cells expressing EPC1-3xFLAG or MBTD1-3xFLAG (as in (A)) (*non-specific band). **(D)** Purified complexes from (B) and (C) were analyzed by western blot with the indicated antibodies to confirm the equivalent presence of known subunits of the TIP60 complex. The doublet appearing with the anti-MBTD1 antibody in the MBTD1-FLAG purification corresponds to inefficient self-cleaving peptide to remove the puromycin resistance portion of the tagged protein (also identified in (A-C)). (**E**) Purification of the TIP60 complex from a cell line expressing a truncated EPC1(1-581)-3xFLAG protein and analyzed as in (A). (**F**) MBTD1 association to TIP60 depends on EPC1 C-terminus. Western blot analysis of EPC1(1-581)-3xFLAG and EPC1-3xFLAG purifications. (**G**) MBTD1 directly interacts with EPC1 C-terminus through its MBT domains. Western blot analysis of GST pulldowns using EPC1 C-terminus (aa582 to 836) incubated with the indicated MBTD1 fragments. (**H**) Schematic representation of EPC1 and MBTD1 functional domains and interactions.

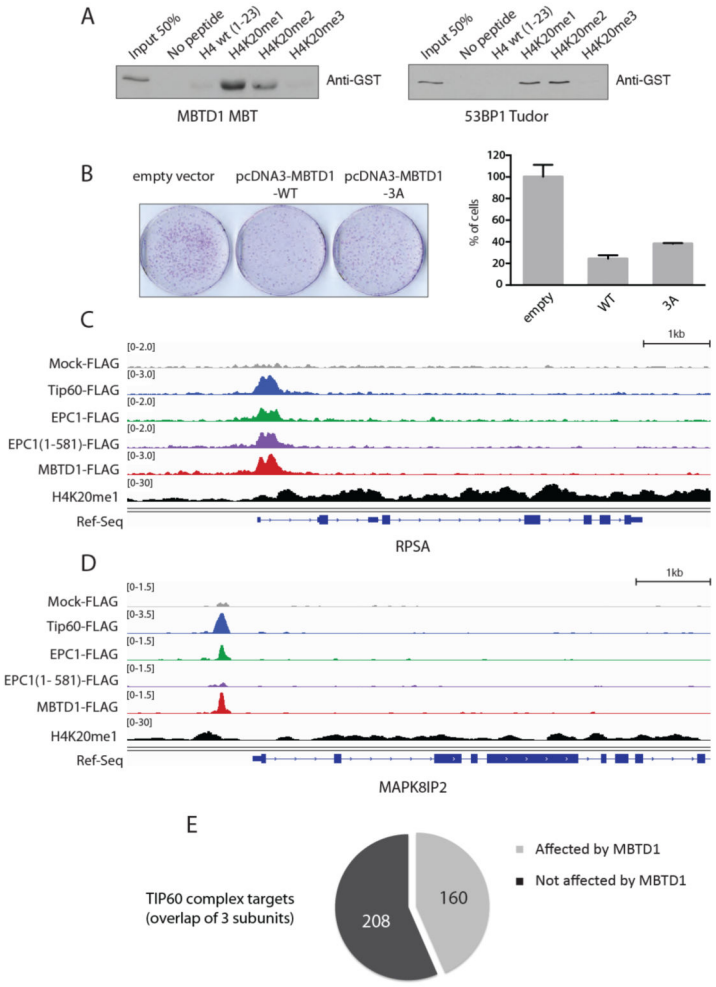

Figure 2. MBTD1 binds the H4K20me1/2 histone mark and colocalizes with the TIP60 complex at gene regulatory elements in the genome

(A) GST-tagged MBT domains of MBTD1 analyzed by peptide pulldown with the indicated biotinylated H4 peptides (aa1 to 23) (left panel); as positive control, the GST-tagged tandem Tudor domain of 53BP1 (aa1484 to 1603) is shown (right panel). Pulldowns were revealed by Western blotting with anti-GST. **(B)** Overexpression of MBTD1 suppresses cell growth by clonogenic assay. A MBTD1 triple-mutant in the fourth MBT domain is also shown. U2OS cells were transfected in triplicates with WT HA-MBTD1 or F526-W529-Y533A mutant (3A mutant) or empty vector for 48h (expression verified in fig. S2B). Hygromycin-resistant colonies were stained with Giemsa. **(C)** MBTD1, Tip60/KAT5 and EPC1 co-localize near the transcriptional start site (TSS) of the actively transcribed RPSA gene. Genome wide MBTD1 localization was analyzed after ChIP-seq and compared to data obtained in parallel with EPC1, EPC1 C-terminal truncation (EPC1(1-581)) and Tip60/KAT5. Anti-FLAG chromatin immuno-precipitations were performed in tagged and mock K562 cell lines used in figure 1. The values correspond to reads per million of total reads (rpm). The H4K20me1 profile presented is from K562 cells in the Encode consortium dataset (direct reads). **(D)** MBTD1 is important for binding of the TIP60 complex on the promoter of the MAPK8IP2 gene. ChIP-seq data at the MAPK8IP2 gene is shown as an

example where the EPC1(1-581) signal is lost compared to wild type EPC1, indicating a specific role of MBTD1 for the association of the TIP60 complex to this region. **(E)** MBTD1 impacts TIP60 complex localization at specific loci within the genome. Common genomic loci strongly bound by EPC1, Tip60/KAT5 and MBTD1 identified 368 high confidence targets of the TIP60 complex in K562 cells (Fig. S2C, Table S3). Comparison with the EPC1(1-581)-3xFLAG signals reveals that 160 out of these 368 *bone fide* TIP60 targets are affected by the absence of MBTD1 from the complex (log10*p*value ≥ 52.66)(Fig. S2D-H for additional analyses/loci).

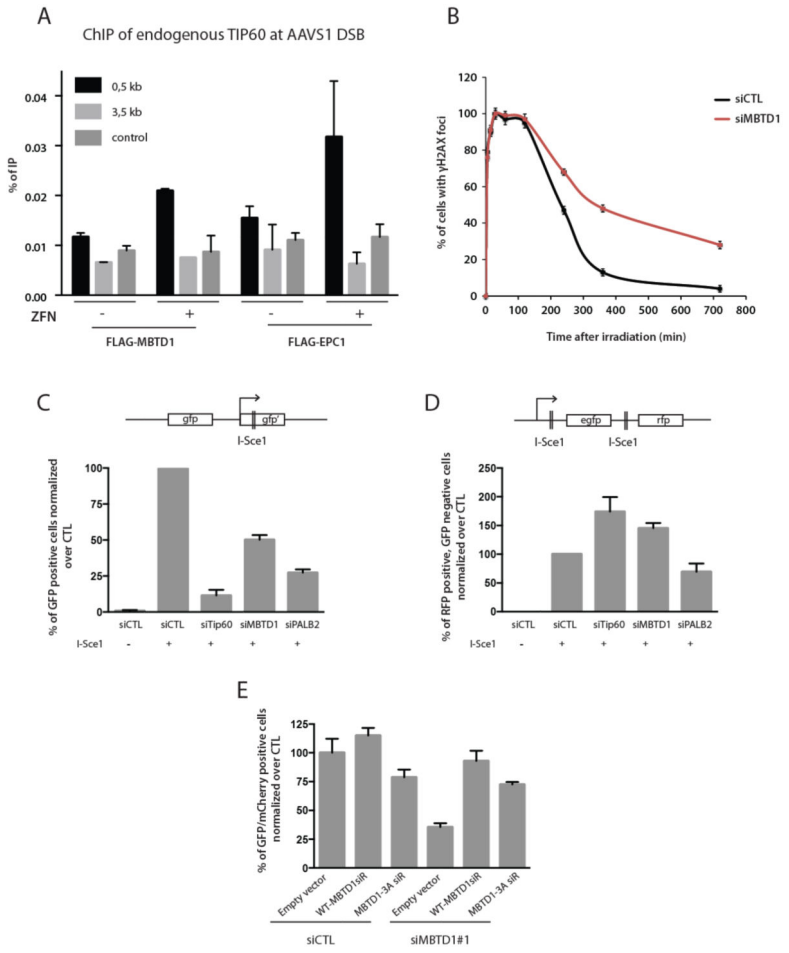

Figure 3. MBTD1 is implicated with TIP60 in the repair of DNA double strand breaks by homologous recombination

(A) MBTD1 is recruited at DNA double strand breaks. K562 cells expressing FLAG-tagged MBTD1 or EPC1 from the endogenous genes (Dalvai et al., 2015) were transfected with a vector expressing a zinc-finger nuclease (ZFN) targeting the *AAVS1* safe harbor followed 18h later by anti-FLAG ChIP. Primers for qPCR are located 0,5 and 3,5kb from the break as well as a negative control locus. Values represent % of input. Error bars are from two independently performed experiments (Fig. S3A for positive control). **(B)** Depletion of MBTD1 affects γ-H2AX foci dynamics after γ-radiations. 293 cells were transfected with the indicated siRNAs for 48h, treated with 2Gy γ-irradiations and processed for γ-H2AX immunofluorescence. Results are presented over time after irradiation as the percentage of cells with more than 4 γ-H2AX foci (mean ± s.e.m, n=3). 100 cells were analyzed for each time-point. Similar results were obtained with shRNAs against other TIP60 subunits and in U2OS cells (Fig. S3C-D). **(C)** Measurement of homology directed repair of an inducible I-Sce1 DSB in U2OS cells using an integrated the DRGFP reporter (schematic on the top). Cells were transfected with the indicated siRNAs for 36h, infected with I-Sce1 adenovirus to induce DSB and then assessed 48h later by FACS analysis for GFP expression. Results represent the percentage of GFP positive cells normalized to the control siRNA, from 2 independent and representative experiments. **(D)** Measurement of I-Sce1 DSB repair by non-

homologous end joining in U2OS cells using an integrated PC222/GFP-RFP reporter (schematic on the top). Cells were treated as in (C) and assessed by FACS for RFP and GFP expression. Results represent the percentage of cells that are RFP positive but GFP negative, normalized to the control siRNA, from 2 independent experiments. **(E)** Complementation assay in the DR-GFP reporter system (from C). Cells were transfected with CTL or MBTD1 siRNAs for 16h, then with pCAG-I-Sce1, pmCherry and siRNA-resistant MBTD1-expressing (WT or 3A mutant F526-W529-Y533A) or empty vectors and finally assessed 48h later by FACS for mCherry and GFP co-expression. Results represent the percentage of mCherry and GFP positive cells normalized to the control siRNA, from 2 independent experiments.

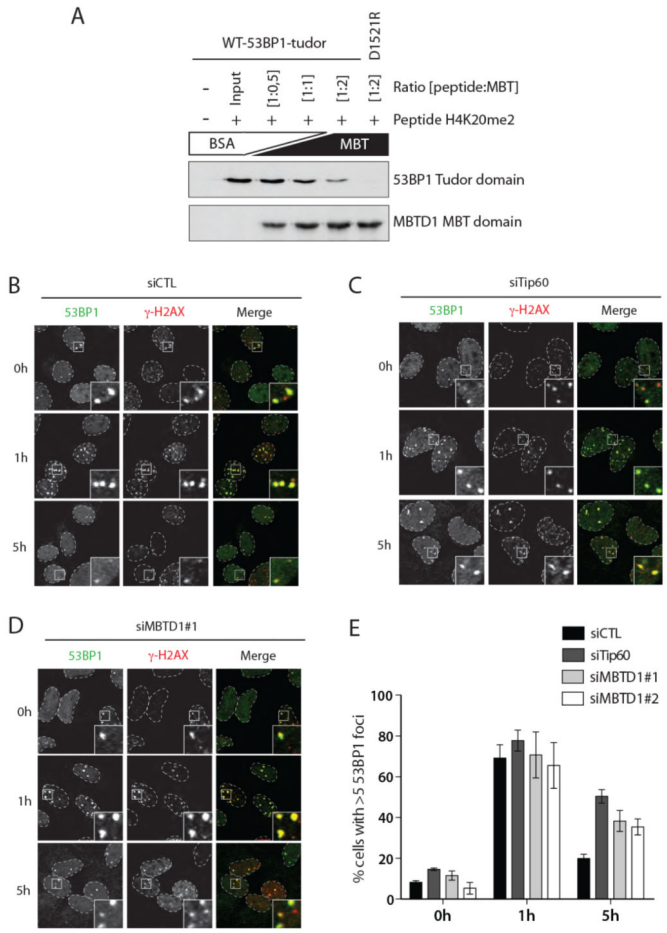

Figure 4. MBTD1 can displace 53BP1 from the H4K20me2 histone mark and affects the dynamics of 53BP1 foci after DNA damage

(A) MBTD1 can remove 53BP1 from H4K20me2 peptides. *In vitro* competition experiment between GST-tagged 53BP1 tandem Tudor domain and MBP-tagged MBTD1 MBT-repeat domain using H4K20me2 peptides (aa1-23). A two-fold excess of 53BP1 tandem Tudor domain (WT or mutant D1521R) was incubated with biotinylated H4 peptide followed by the addition of increasing amounts of purified MBT-repeat domain of MBTD1 (or BSA). The level of binding by the tandem Tudor vs the MBT-repeat was measured by western blot on the peptide bound material using anti-GST or anti-MBP, respectively. **(B) (C)** Tip60/KAT5 affects the dynamics of 53BP1 foci after DNA damage. U2OS cells were transfected with control siRNA (B) or siTip60 (C) and irradiated (2Gy) 48h post-transfection. Cells were processed for γ-H2AX and 53BP1 immunofluorescence 0, 1 and 5h after irradiation. **(D)** MBTD1 knock down phenocopies Tip60 effect on the stability of 53BP1 foci. **(E)** Quantification of the dynamics of 53BP1 foci appearance/disappearance after irradiation in control conditions or when Tip60/MBTD1 are depleted. Data are presented as percentage of cells with more than five 53BP1 foci (mean ± s.d, n=2). Two independent siRNAs for MBTD1 were used (Fig. S3E and S4).

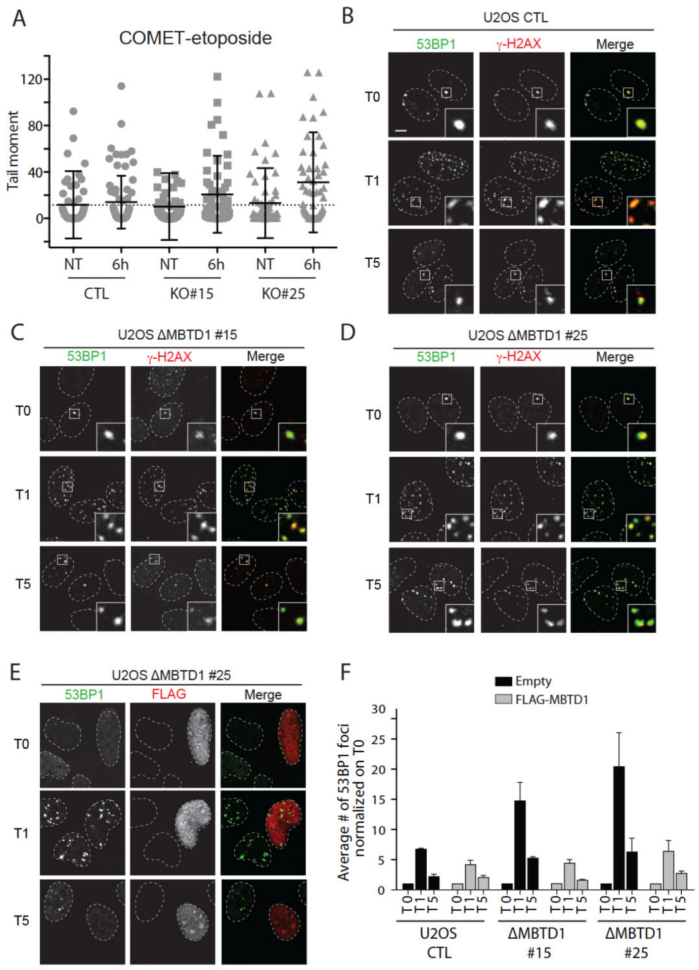

Figure 5. MBTD1 knockout cells show DNA repair deficiency and increased formation of 53BP1 foci after DNA damage

(A) Alkaline comet assay of MBTD1 WT or KO cells (U2OS), non-treated and 6h after etoposide treatment (50μM, 15min). One representative experiment on 2 different KO clones compared to WT (n>60 per condition, mean ± s.d., p=0.0006). Tail moments 30min after treatment are similar in WT and KO cells with a mean around 100. **(B) (C) (D)** Dynamics of IR-induced 53BP1 foci in MBTD1 WT and KO cells. U2OS control cells (B) or KO clones # 15 (C) and #25 (D) were irradiated (2Gy) and processed for γ-H2AX and 53BP1 immunofluorescence 0, 1 and 5h after irradiation (scale bar is 5μm). **(E)** Re-introduction of MBTD1 in KO cells restores 53BP1 foci dynamics. KO cells (#25 is shown) were transfected with empty vector or FLAG-MBTD1, irradiated (2Gy) 24h post-transfection and processed for FLAG and 53BP1 immunofluorescence 0, 1 and 5h after irradiation. **(F)** Quantification of (B) (C) (D) and rescue experiment (E). At each time point, the number of 53BP1 foci was counted in at least 50 cells, averaged and normalized against the average number of foci counted in the same cell line at time 0 (T0 = 1). (means ± s.e.m., n = 3; rescue: means ± s.e.m., n ≥ 2).

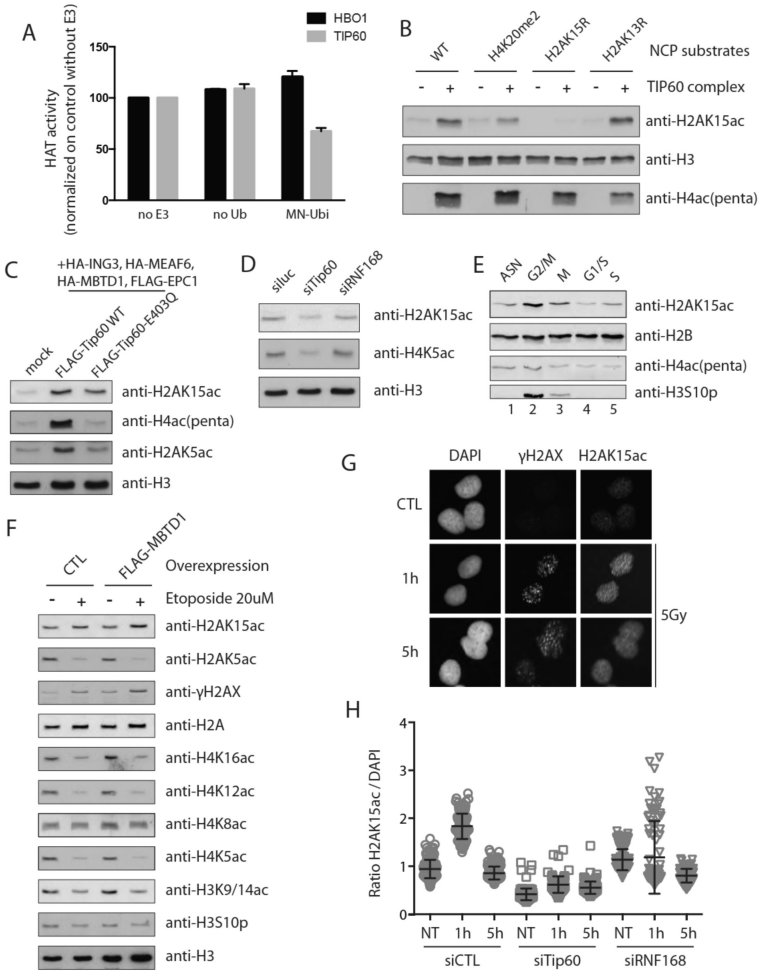

Figure 6. H2AK15 ubiquitylation by RNF168 versus acetylation by the TIP60 complex

(A) H2A ubiquitylation by RNF168 specifically inhibits TIP60-dependant acetylation of nucleosomes. Native mononucleosomes from HeLa cells were ubiquitylated *in vitro* with RNF168/E1/E2 (500ng; Fig. S6A) and used as substrate in HAT assays with purified TIP60 complex. Another histone H4-specific HAT complex, HBO1, was used as control. Values are normalized on the activity measured on control nucleosomes prepared without RNF168 (mean ± s.d, n=2). **(B)** H2AK15 is acetylated by the TIP60 complex on nucleosomes *in vitro*; validation of H2AK15ac antibody specificity and interrelation with H4K20me2. Recombinant mononucleosomes (NCP) were used as substrates with purified TIP60 complex (EPC1-3xFLAG, Fig. 1). Wild type and mutant NCPs were used as well as one carrying H4Kc20me2 (methyllysine analog). **(C)** H2AK15 is a substrate of TIP60 *in vivo*. Chromatin was extracted from 293T cells transfected with a nucleosomal HAT sub-complex of TIP60 (piccolo-TIP60/NuA4) containing EPC1, ING3, MEAF6, MBTD1 and wild type Tip60 or the enzymatically dead E403Q mutant (Fig. S6C). H2AK15, H2AK5ac, H4ac and H3 signals were analyzed by western blotting. **(D)** Tip60 knockdown affects H2AK15ac level *in vivo*. Acid extracted histones from U2OS cells transfected with the indicated siRNAs for 48h were analyzed by western blotting for different histone modifications. **(E)** Acetylation of H2AK15 is regulated during the cell cycle. H2AK15 acetylation was

analyzed by western blotting in U2OS cells synchronized by double-thymidine block and release (lanes 4 & 5; 0 and 2h, respectively) or thymidine-nocodazole block and release (lanes 2 & 3; 0 and 30 min, respectively). Asynchronous cells are shown as control (lane 1, ASN) and H3S10p signal is shown as G2/M marker (Fig. S6F for FACS). **(F)** H2AK15ac is differentially regulated in response to DNA damage. Acid extracted histones from 293T cells transfected with MBTD1 or control vector and treated or not with etoposide (20μM, 1h) were analyzed by western blotting for different histone modifications. **(G)** Nuclear H2AK15ac increases after DNA damage. U2OS cells were irradiated with 5 Gy, processed after 0, 1 or 5h for H2AK15ac and γ-H2AX immunofluorescence and DAPI. **(H)** H2AK15ac increase upon DNA damage is dependent on Tip60. U2OS cells were irradiated with 5 Gy, 48h post transfection with the indicated siRNAs, and processed after 0, 1 or 5h for H2AK15ac immunofluorescence and DAPI. H2AK15ac signals were normalized on the DAPI signal in the same nuclei ($n>80$ per condition in duplicate, mean ± s.d, $p<0.0001$).

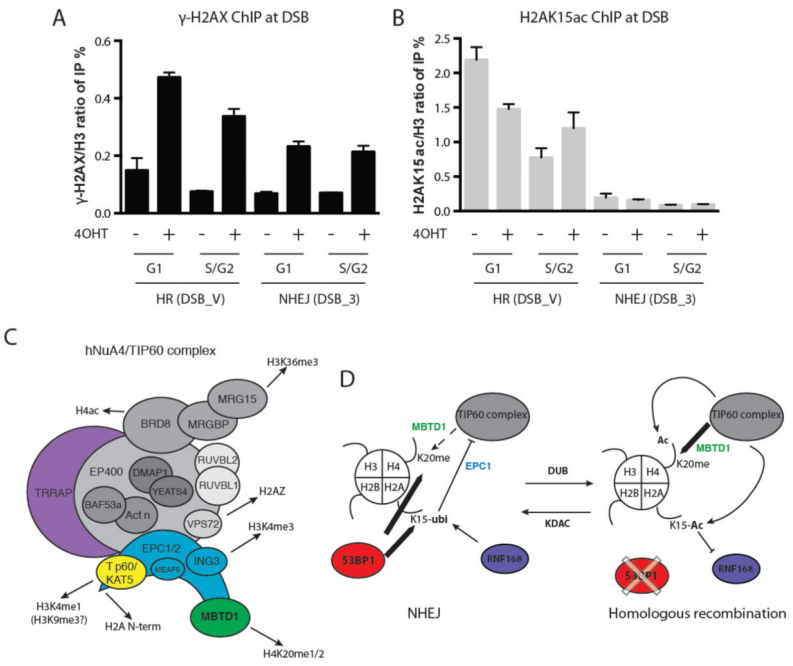

Figure 7. Acetylation of H2AK15 by TIP60 is linked to breaks preferentially repaired by HR during S/G2

(A) (B) H2AK15 is acetylated at pro-HR DSB in S/G2 cells. γ-H2AX and H2AK15ac ChIP experiments in AID-DIvA cells (Aymard et al., 2014) after synchronization by double thymidine block and treatment with 4-OHT. Results are normalized for nucleosome occupancy over H3 IP % and represent a duplicate of independent experiments (Fig. S7B for other DSB sites). **(C)** Schematic representation of TIP60 complex composition and its multiple histone mark reader subunits that regulate its interaction with chromatin. **(D)** Model for TIP60 regulation of 53BP1 during DSB repair pathway choice. TIP60 regulates DSB repair pathway selection by sharing common nucleosomal histone targets with 53BP1 on nucleosomes and by creating an ubiquitylation / acetylation switch at H2AK15. MBTD1 and 53BP1 both target H4K20me2 which promotes their binding to chromatin. RNF168 ubiquitylates H2AK15 in response to DNA damage to recruit 53BP1 on damaged chromatin. During NHEJ, H2AK15 ubiquitylation blocks TIP60 (EPC1) binding to the H2A tail and H4 acetylation, favoring 53BP1 retention at the break and inhibition of resection. On the other hand, TIP60 acetylates H2AK15 and therefore blocks ubiquitylation by RNF168 and 53BP1 binding. This can prevent promiscuous DNA damage-induced ubiquitylation of H2A throughout the genome, but also participates with H4K20me2 binding and H4 acetylation by TIP60/MBTD1 in disrupting 53BP1 occupancy on damaged chromatin to allow resection and repair by homologous recombination. The action of specific deubiquitinase (DUB) and deacetylases (KDAC) will be important to determine which interactions and modifications are favored on specific nucleosomes.